International Journal of Civil Engineering

Water Hydrology

Technical Note

Applying digital image correlation method to measure flow field

J-Ch Kuo [1], Sh-H Tung[2], M-H Shih[3], W-P Sung[4,*], T-Y Kuo[1], Ch-H Wu[1], W-S Hwang[1]

Received: July 2012, Revised: November 2013, Accepted: January 2014

Abstract

In this study digital image correlation (DIC) technique combined with a high speed video system was used to predict movement of particles in a water model. Comparing with Particle-image velocimetry (PIV) technique, it provides a low cost alternative approach to visualize flow fields and was successfully employed to predict the movement of particles in a water model at different submergence depth using gas injection. As the submergence depth increases, the number of the exposed eye is reduced accordingly. At 26.4 cm submergence depth, an exposed eye was found at 1/3 of the submergence depth, whereas two exposed eyes were observed at 1/2 depth and near the bottom wall at 24 cm submergence depth.

Keywords: *Digital image correlation (DIC), Fluid flow, Water model, Mixing.*

1. Introduction

Particle-image velocimetry (PIV) is a well-established technique for quantitative measurement of velocity fields in macroscopic scale [1-11]. In the case of double-pulsed PIV, the particles are illuminated either using a pulsed light source, or using a continuous light source. It is based on measuring displacements of scattering particles between successive exposures, which is usually recorded photographically. The displacement of the particle images is then estimated statistically by correlating the particle image pairs [2]. Thus, the whole two-dimensional flow field can be measured simultaneously by PIV without disturbing the flow field. After the first studies, many investigations have been focused at improving its performances [1,12,4], including the cross correlation technique [1] and four-step particle tracking [13]. A very important step was the introduction of the digital recording and treatment of PIV images [12]. In 1998 Santiago et al [3] conducted the first successful micro-PIV experiment for investigating flows around living microorganisms.

In the last decade, optical digital image techniques for strain measurement have advanced significantly because of the availability of cheap and powerful digital imaging and data processing hardware.

Therefore, these advantages enable the digital image correlation (DIC) technique to be widely applied in determination of two-dimensional displacement field, such as the observation of cracks in the brick wall [14] and the monitoring of bridges and full-size building elements [14,16]. The measured displacement field using DIC technique is based on the image correlation function, which determines the degree of similarity between two digital images of the specimen surface before and after deformation. Therefore, in the present study, the optical digital image technique combined with a high speed CCD camera was employed to visualize the flow fluid in a water model to understand inclusion movement. Comparing with PIV, it provides an alternative method to determine the flow fluid at low cost simple setup.

Understanding the gas bubble and inclusion movement in liquid steel is important to remove and control steel quality and properties using gas injection [17-21]. Here a water model was employed to simulate the condition of liquid steel using the gas injection. In addition the behavior of inclusion movement was predicted by tracing the particles in the water model.

2. Methodology

Digital Image Correlation method is basically taken as the foundation of "search to perform mathematical calculations ", comparing the partial relativity of two images and judging the image towards reflection before and after transformation. This concept, which makes use of finite element method, will transform in-front and back.

** Corresponding author: wps@ncut.edu.tw*
1 Department of Materials Science and Engineering, National Cheng-Kung University, Tainan 701, Taiwan
2 Department of Civil and Environmental Engineering, National University of Kaohsiung, Kaohsiung 811, Taiwan
3 Department of Construction Engineering, National Chi Nan University, Nan-Tou 545, Taiwan
4 Department of Landscape Architecture, National Chin-Yi University of Technology, Taichung 411, Taiwan

It attempts to divide the image body up into a small mesh, being called as sub-image. Assuming the one point of sub-image, which transforms an in-front and back bit in a displacement function:

$$x^* = x + u(x, y)$$
$$y^* = y + v(x, y) \quad (1)$$

The relativity analysis related to transforming in-front and back is in accordance with the Digital Image Correlation method that judges the degree of transforming the image in-front and back. This makes the sum of the gray scale inside image equal to the total amount. The Digital Image Correlation method is defined as follows:

$$COF = \frac{\Sigma g_{ij} \tilde{g}_{\bar{i}\bar{j}}}{\sqrt{\Sigma g_{ij}^2 \cdot \Sigma \tilde{g}_{\bar{i}\bar{j}}^2}} \quad (2)$$

Where, g_{ij} and $\tilde{g}_{\bar{i}\bar{j}}$ are grey scale of image A on coordinate (i, j) and image B on coordinate $(\bar{i}, \bar{j})$, respectively. And coordinate $(\bar{i}, \bar{j})$ of image B corresponds to coordinate (i,j) of image A.

If optimal function parameters for every sub-image are recognized, the corresponding coordinates of every deformed or un-deformed sub-image can be obtained. Accordingly, the displacement and strain field can be computed individually.

3. Experimental Setup

The fluid flow in a water model was visualized using DIC. The water model was represented by a transparent vessel of plexi-glass. During gas injection, a series of digital images were recorded to determine the fluid flow in the water model.

The set-up for the determination of fluid flow (Fig. l) consisted of a cylindrical plexi-glass vessel that contained tap water at room temperature. The vessel was 100 mm wide, 270 mm high, and 2 mm thick. Before injection, 300,000 spherical particles of low-density polyethylene with a density of 0.92 g/cm^3 were on the top surface. Using a compressor, air was injected through a centric top nozzle into the bath at a flow rate of 4 L/min. The nozzle, having an inner diameter of 1.2 mm and an outer diameter of 5.0 mm, was located at 26.4 and 24 cm below the top surface, respectively.

To simulate a quasi-2D projected area, light was limited to pass through two narrow parallel planes (Fig. 1). A high speed video system, NAC Memrecam GX 3 with a 520 × 512 pixel resolution, was employed to capture 750 frames per s after 10 s injection time.

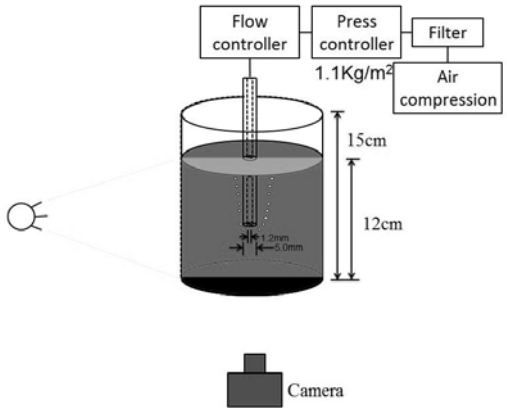

Fig. 1 The schematic set up of flow field measurement for a water model

4. Results and Discussion

4.1. Determination of fluid flow

In the current study, a new method to measure the fluid flow using DIC combined with high speed video system was proposed. Examples of the injection process at depths of 26.4 and 24 cm are shown in Fig. 2. An asymmetrical plume zone consisting of injected gas bubbles was observed at the center of the image in both cases. The dynamic shape changes of the resultant gas bubbles hindered the tracing of the bubble movement. Therefore, the images for DIC measurements were captured on the areas without the gas bubbles.

Figs. 3(a) and (b) show the serial photos captured by the high speed video system after a time interval of 1/750 s in which Fig 3(a) was used as a reference image. The negative images of the original images [Figs. 3(c) and (d)] were produced. After the negative image processing, the analyzed area of the reference image was marked with the 32 × 32 pixel grid [Fig. 4(a)]. The procedure for DIC analysis was described in the authors' previous study where the resolution of this technique was set at approximately 10^{-4} [17, 18]. Using DIC, the new positions in the marked area after 1/750 s were calculated in Fig. 4(b). The displacement of each point in Fig. 4(c) was determined, and the displacement distribution in the analyzed area is presented in Fig. 4(e). The fluid velocity at each point was obtained by dividing the displacement with the interval time.

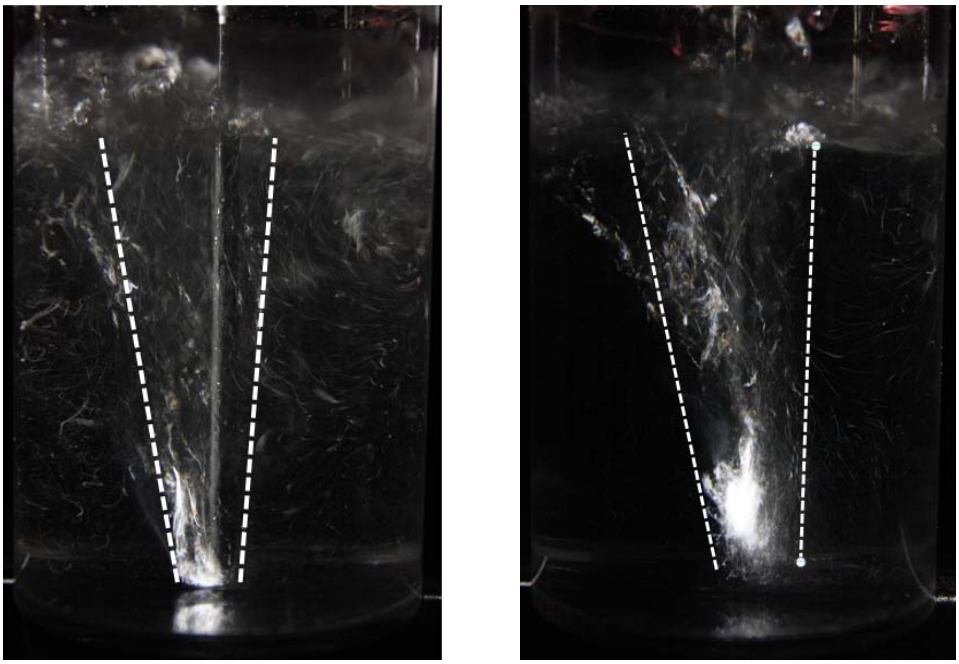

(a) (b)

Fig. 2 Flow pattern for vertical injection direction at (a) 26.4 and (b) 24 cm submergence below the water surface. The dashed line represents the plume zone

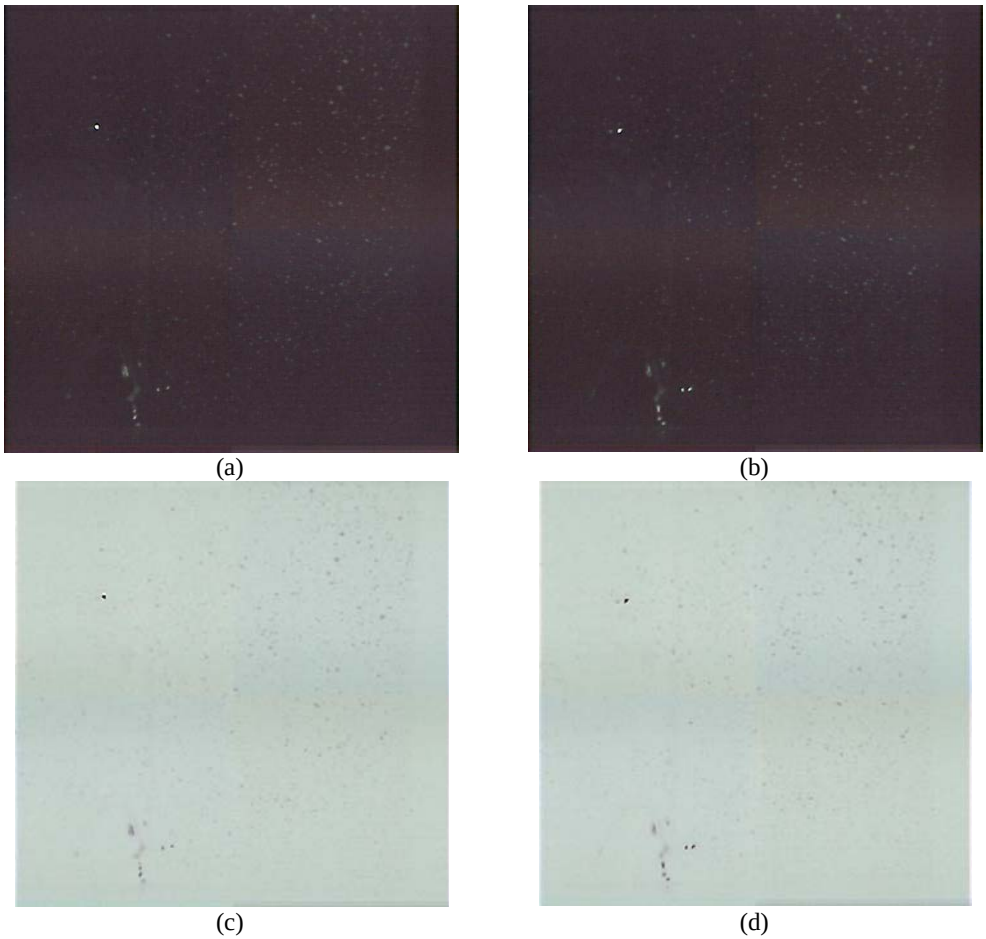

(a) (b)

(c) (d)

Fig. 3 (a) The reference image and (b) an analyzed image after 1/750 s, whereas (c) and (d) are the negative images of (a) and (b), respectively

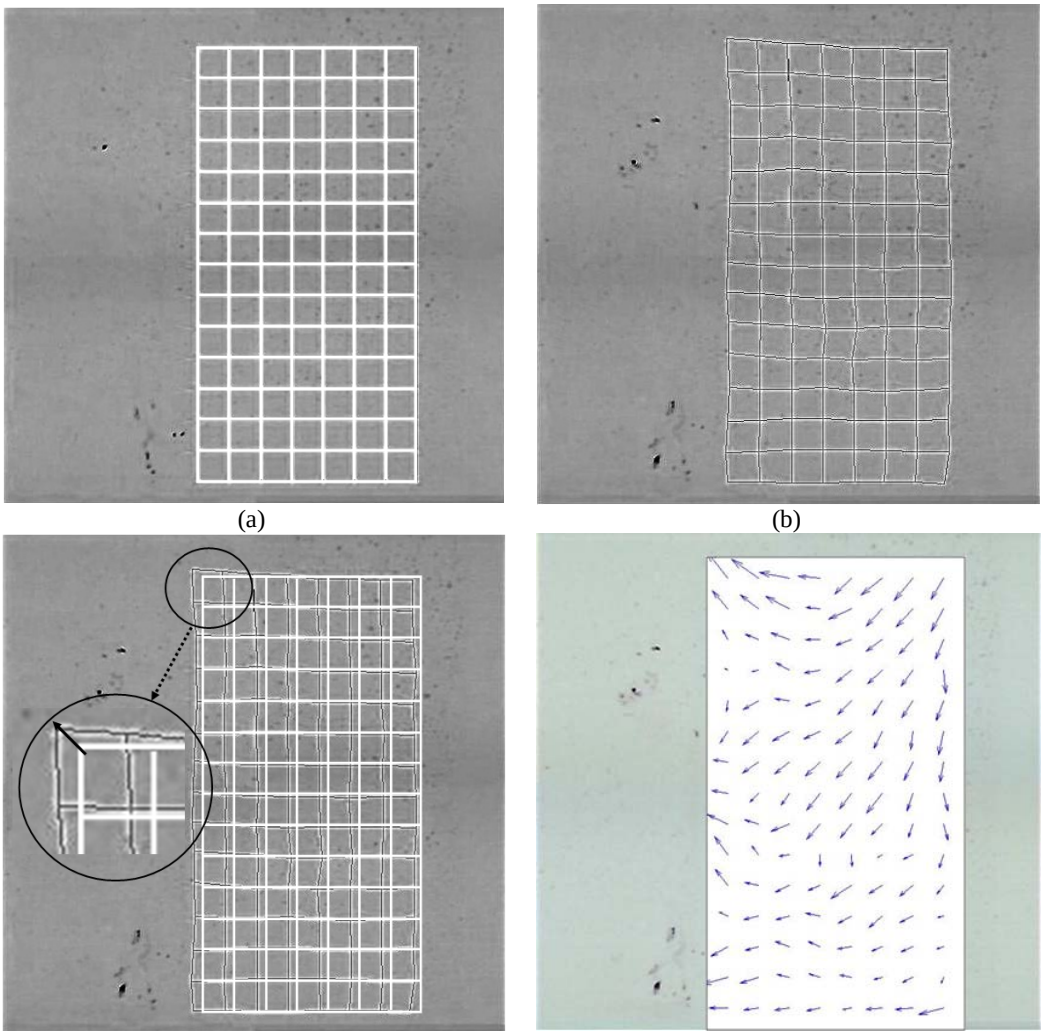

Fig. 4 (a) The initial grid in the reference image, (b) the grid in the analyzed image after 1/750 s obtained using DIC, (c) the analyzed image that overlapped with the initial grid, and (d) the flow field distribution in the analyzed image obtained using DIC

4.2. Effect of the submergence depth on the flow pattern

The flow patterns for the injection process at the submergence depths of 26.4 and 24 cm are shown in Figs. 2(a) and 2(b), respectively. A plume zone is asymmetrical about the centric nozzle in the middle area for both cases. In this zone, the carrier gas rises to the free surface and induces recirculation flows of fluid within the vessel. According to the macroscopic plume model proposed by Sahai and Guthrie [19], the average velocity of a plume, U_P, is estimated by

$$U_p = k \cdot Q^{1/3} L^{1/4} / R^{1/3} \quad (3)$$

where Q is the gas flow, L is the liquid depth, and R is the ladle radius. According to Equation (1), an increase in the nozzle depth causes the recirculation speeds to increase.

In addition to the plume zone, flow fields were visualized using 2D DIC by scanning a plane near the nozzle [Figs. 5(b) and 6(b)]. At 26.4 cm depth, an exposed eye was created at 1/3 of the submergence depth in Fig. 5(b). The position of the eye corresponds to that in the flow pattern after prolonged exposure obtained from a CCD camera in Fig. 5(a). The velocity vectors were almost pointing toward the nozzle. The bubbles near the nozzle had enough buoyant force to rise to the free surface of water. These rising bubbles created upward flows and formed the exposed eye.

For the 24 cm depth, two exposed eyes were observed at 1/2 depth and at the bottom [Fig. 6(b)]. The size of the upper exposed eye at 24 cm depth was smaller than that at 26.4 cm depth [Figs. 5(a) and 6(a)]. The lower part of Figure 6(b) shows upward flows near the outlet port. These upward flows produced the recirculation as marked with the lower exposed eye. Compared with that at 24 cm depth, this recirculation was limited because of the small distance between the outlet and the bottom wall. Therefore, no low exposed eye was observed.

In summary, in this study, the DIC technique was

successfully applied to predict the movement of particles in a water model. The results are important to understanding the gas bubble and inclusion movement in liquid steel in order to remove and control steel quality and properties using gas injection. The approach also provides a low cost method to determine the flow fluid in a water model.

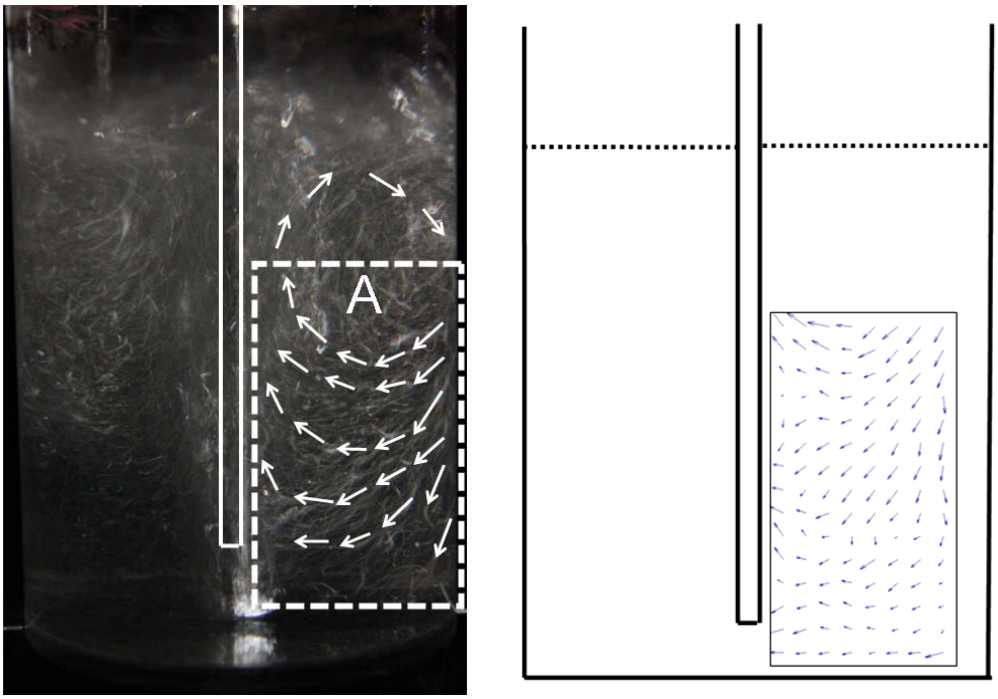

(a) (b)

Fig. 5 (a) The flow pattern after prolonged exposure using a CCD camera and (b) the flow field map using DIC analysis with a high speed video system at 26.4 cm submergence depth.

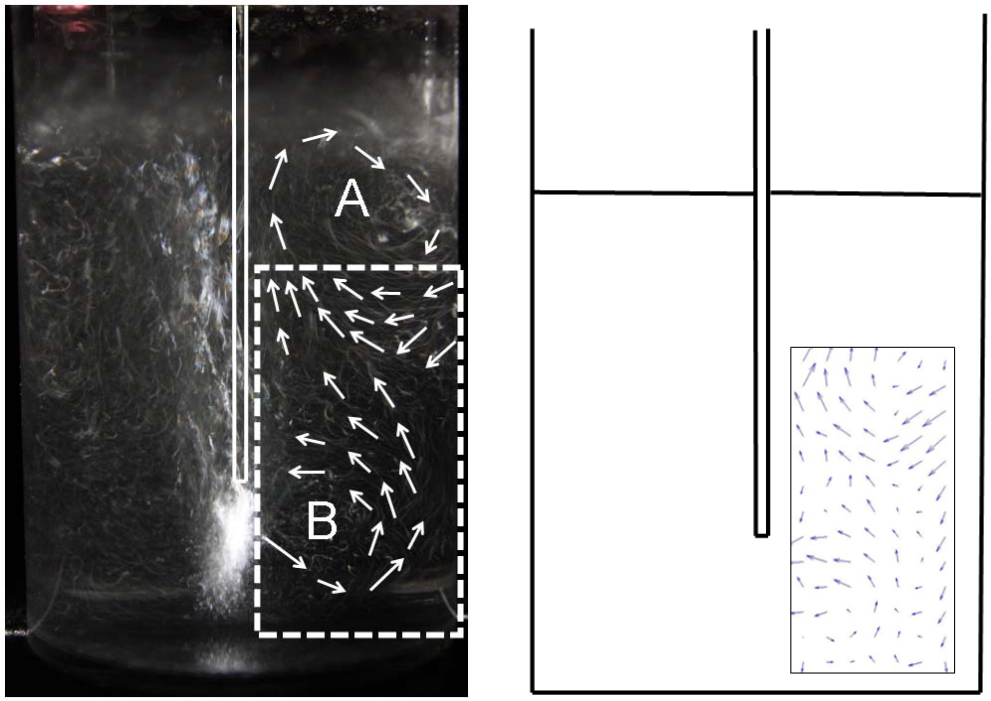

(a) (b)

Fig. 6 (a) The flow pattern after prolonged exposure using a CCD camera and (b) the flow field map using DIC analysis with a high speed video system at 24 cm submergence depth

5. Conclusions

In this investigation, DIC technique combined with a high speed video system provides a low cost alternative approach to visualize flow fields in a water model. It was successfully applied to predict the movement of particles in a water model. At 26.4 cm submergence depth, an exposed eye was found at 1/3 of the submergence depth. At 24 cm submergence depth, two exposed eyes were formed at 1/2 of the submergence depth and near the bottom wall.

References

[1] Adrian RJ. Particle-imaging techniques for experimental fluid-mechanics, Annual Review of Fluid Mechanics, 1991, Vol. 23, pp. 261-304.

[2] Meinhart CD, Prasad AK, Adrian RJ. A parallel digital processor for particle image velocimerty, Measurement Science and Technology, 1993, Vol. 4, pp. 619-626.

[3] Santiago JG, Wereley ST, Meinhart CD, Beebe DJ, Adrian RJ. A particle image velocimetry system for microfluidics, Experiments in Fluids, 1998, Vol. 25, pp. 316-319.

[4] Huang HT, Fiedler HE, Wang JJ. Limitation and Improvement of PIV .2. particle image distortion, a novel technique, Experiments in Fluids, 1993, Vol. 15, pp. 263-273.

[5] Lourenco L, Krothapalli A. On the accuracy of velocity and vorticity measurements with PIV, Experiments in Fluids, 1995, Vol. 18, pp. 421-428.

[6] Westerweel J, Dabiri D, Gharib M. The effect of a discrete window offset on the accuracy of cross-correlation analysis of digital PIV recordings, Experiments in Fluids, 1997, Vol. 23, pp. 20-28.

[7] Zhang J, Tao B, Katz J. Turbulent flow measurement in a square duct with hybrid holographic PIV, Experiments in Fluids, 1997, Vol. 23, pp. 373-381.

[8] Scarano F, Riethmuller ML. Iterative multigrid approach in PIV image processing with discrete window offset, Experiments in Fluids, 1999, Vol. 26, pp. 513-523.

[9] Meinhart CD, Wereley ST, Santiago JG. PIV measurements of a microchannel flow, Experiments in Fluids, 1999, Vol. 27, pp. 414-419.

[10] Meinhart CD, Wereley ST, Santiago JG. A PIV algorithm for estimating time-averaged velocity fields, Journal of Fluids Engineering, Transactions of the ASME, 2000, Vol. 122, pp. 285-289.

[11] Okamoto K, Nishio S, Saga T, Kobayashi T. Standard images for particle-image velocimetry, Measurement Science and Technology, 2000, Vol. 11, pp. 685-691.

[12] Willert CE, Gharib M. Digital particle image velocimetry, Experiments in Fluids, 1991, Vol. 10, pp. 181-193.

[13] Kobayashi T, Saga T, Segawa S, Knada H. Trans. JSME B 55 107, 1989.

[14] Tung SH, Shih MH, Sung WP. Development of digital image correlation method to analyze crack variations of masonry wall, Sadhana -Academy Proceedings in Engineering Science, 2008, Vol. 33, pp. 767-779.

[15] Lee JJ, Shinozuka M. Real-time displacement measurement of a flexible bridge using digital image processing techniques, Experimental Mechanics, 2006, Vol. 46, pp. 105–114.

[16] Lee WT, Chiou YJ, Shih MH. Reinforced concrete beam-column joint strengthened with carbon fiber reinforced polymer (CFRP), Composite Structures, 2010, Vol. 92, pp. 48-60.

[17] Zhang L, Taniguchi S. Fundamentals of inclusions removal from liquid steel by bubbles flotation, International Materials Reviews, 2000, Vol. 45, 59-82.

[18] Iguchi M, Yoshida J, Shimizu T, Mizuno Y. Model study on the entrapment of mold powder into molten steel, ISIJ Interanational, 2000, Vol.40, pp. 685-691.

[19] Wang Z, Mukai K, Ma ZY, Nishi M, Tsukamoto H, Shi F. Influence of injected ar gas on the involvement of the mold powder under different wettabilities between porous refractory and molten steel, ISIJ International, 1999, Vol. 39, pp. 795-803.

[20] Mazumdar D, Guthrie RIL. The physical and mathematical-modeling of gas-stirred ladle systems, ISIJ International, 1995, Vol. 35, pp. 1-20.

[21] Murthy GGK. Mathematical-modeling and simulation of recirculatory flow as well as mixing phenomena in gas stirred liquid baths, ISIJ International, 1989, Vol. 29, pp. 49-57.